AMERICAN SOCIETY of
GENE & CELL
THERAPY

HIF-1α Dependent Wound Healing Angiogenesis In Vivo Can Be Controlled by Site-Specific Lentiviral Magnetic Targeting of SHP-2

Yvonn Heun,[1,7,9] Kristin Pogoda,[1,9] Martina Anton,[2] Joachim Pircher,[3,7] Alexander Pfeifer,[4] Markus Woernle,[5] Andrea Ribeiro,[5] Petra Kameritsch,[1] Olga Mykhaylyk,[2] Christian Plank,[2] Florian Kroetz,[6] Ulrich Pohl,[1,7,8] and Hanna Mannell[1,7]

[1]Walter Brendel Centre of Experimental Medicine, BMC, Ludwig-Maximilians-University, Grosshaderner Strasse 9, 82152 Planegg, Germany; [2]Institut für Molekulare Immunologie - Experimentelle Onkologie, Klinikum rechts der Isar der TUM, Ismaninger Strasse 22, 81675 München, Germany; [3]Medizinische Klinik und Poliklinik I, Klinikum der Universität München, Marchioninistrasse 15, 81377 Munich, Germany; [4]Institute of Pharmacology and Toxicology, Biomedical Center, University of Bonn, Sigmund-Freud-Strasse 25, 53105 Bonn, Germany; [5]Medizinische Klinik und Poliklinik IV, Klinikum der Universität München, Ziemssenstrasse 1, 80336 Munich, Germany; [6]Interventional Cardiology, Starnberg Community Hospital, Osswaldstrasse 1, 82319 Starnberg, Germany; [7]DZHK (German Center for Cardiovascular Research) partner site Munich Heart Alliance, 81377 Munich, Germany; [8]Munich Cluster for Systems Neurology, (SyNergy), 81377 Munich, Germany

Hypoxia promotes vascularization by stabilization and activation of the hypoxia inducible factor 1α (HIF-1α), which constitutes a target for angiogenic gene therapy. However, gene therapy is hampered by low gene delivery efficiency and non-specific side effects. Here, we developed a gene transfer technique based on magnetic targeting of magnetic nanoparticle-lentivirus (MNP-LV) complexes allowing site-directed gene delivery to individual wounds in the dorsal skin of mice. Using this technique, we were able to control HIF-1α dependent wound healing angiogenesis in vivo via site-specific modulation of the tyrosine phosphatase activity of SHP-2. We thus uncover a novel physiological role of SHP-2 in protecting HIF-1α from proteasomal degradation via a Src kinase dependent mechanism, resulting in HIF-1α DNA-binding and transcriptional activity in vitro and in vivo. Excitingly, using targeting of MNP-LV complexes, we achieved simultaneous expression of constitutively active as well as inactive SHP-2 mutant proteins in separate wounds in vivo and hereby specifically and locally controlled HIF-1α activity as well as the angiogenic wound healing response in vivo. Therefore, magnetically targeted lentiviral induced modulation of SHP-2 activity may be an attractive approach for controlling patho-physiological conditions relying on hypoxic vessel growth at specific sites.

INTRODUCTION

Angiogenic gene therapy shows great potential in improving ischemic cardiovascular disease[1,2] and wound healing,[3] while anti-angiogenic gene therapy is a promising approach to inhibit tumor growth[4] and ocular disease.[5] The main hurdles with this technique yet to overcome are poor gene delivery and expression efficiency at the desired site and non-specific distribution of the therapeutic genes. Due to their low immunogenicity, high efficiency in transfecting non-dividing cells, and long-term expression profile, lentiviruses may represent an effective gene delivery system for endothelial and thus angiogenic gene

therapy. By combining therapeutic lentiviral vectors with a targeting system, therapeutic gene expression exclusively at desired sites may be achieved and non-specific distribution prevented. Superparamagnetic nanoparticles (MNP) have been shown to successfully target DNA vectors or small interfering (si)RNA to several cell types and tissues upon magnetic field exposure[6–8] and show favorable characteristics for in vivo application, such as low cytotoxicity.[9] Magnetically guided lentiviral gene delivery, using MNP associated to lentiviruses, has repeatedly been used by us to efficiently transfect cells in vitro and target reporter gene expression in vivo.[10–12] Thus, lentiviral MNP may represent an efficient approach to manipulate physiological processes in vivo. However, magnetic targeting of therapeutic lentiviral MNP has not yet been tested for its ability to specifically control angiogenesis in vivo.

A condition, which is a strong inducer of angiogenesis thereby influencing for instance wound healing, tumor growth, and diabetic retinopathy,[13,14] is hypoxia. The responsible factor for these angiogenic responses is the transcription factor hypoxia inducible factor 1 (HIF-1), consisting of the subunits HIF-1α and HIF-1β. In a normoxic environment, HIF-1α is rapidly degraded by the proteasome due to hydroxylation of two proline residues by the prolyl hydroxylase domain containing enzymes (PHD). Under hypoxic conditions, HIF-1α accumulates and induces expression of several angiogenic genes through binding to hypoxia responsive elements

CrossMark

(HRE) in the promotor region.[14,15] Due to the absolute importance of HIF-1α within this context, it has been the target of therapeutic strategies aiming at either inducing vessel growth, as in the case of diabetic wound healing[16,17] and limb ischemia,[18] or inhibiting vessel formation to impair tumor growth[19,20] or retinal neovascularization.[21] Therefore, factors regulating HIF-1α expression or activity may in addition be of interest for therapeutic approaches. Previously, we showed that the tyrosine phosphatase SHP-2 regulates growth factor dependent vessel formation,[22] and in an earlier study, Saxton et al.[23] found SHP-2 to influence the formation of the vascular network of the yolk sac in mice embryos. However, it is still unknown if SHP-2 plays a role in hypoxic angiogenesis. In addition, an influence of SHP-2 on HIF-1α stabilization and activation has never been investigated. Furthermore, no studies regarding the potential of SHP-2 as therapeutic target for angiogenic therapy has been performed.

Therefore, we established an in vivo model, where complexes of therapeutic lentiviruses and MNP were targeted to individual sites within the same tissue to differentially influence wound healing angiogenesis and to study the role of SHP-2 in this process. We found SHP-2 to be essential for hypoxic angiogenesis by inhibiting HIF-1α degradation through Src activation resulting in HIF-1α DNA-binding and transcriptional activity in vitro as well as in vivo. Excitingly, by using complexes of lentiviral vectors and magnetic nanoparticles, we induced the simultaneous expression of constitutively active as well as inactive SHP-2 mutant proteins in separate wounds within the same tissue in mice, thus specifically and locally controlling the response to wound healing angiogenesis and HIF-1α activity in vivo. Thus, magnetic site-directed genetic modulation of SHP-2 activity may constitute a potent approach to empower controlled modulation or fine-tuning of angiogenesis at specific sites.

RESULTS

Loss of SHP-2 Phosphatase Activity Impairs Angiogenesis and HIF-1α Stabilization under Hypoxic Conditions In Vitro

To investigate the influence of SHP-2 on angiogenic processes under hypoxia, endothelial cells were lentivirally transduced with myc-tagged SHP-2 wild-type (WT), a dominant negative SHP-2 mutant (CS), where the critical cysteine 459 in the phosphatase domain was exchanged for serine, or a constitutively active SHP-2 (E76A) (Figure S1). Endothelial cells overexpressing SHP-2 CS showed a significantly impaired proliferation during hypoxic conditions, whereas overexpression of SHP-2 E76A resulted in enhanced proliferation compared to cells overexpressing the SHP-2 WT construct ($p < 0.05$, n = 5 in triplicates; Figure 1A). However, treatment of SHP-2 E76A cells with the HIF-1α inhibitor echinomycin[24] prevented the increase in proliferation previously observed in these cells ($p < 0.05$, n = 5 in triplicates). Moreover, expression of SHP-2 CS significantly reduced the formation of capillary like structures in Matrigel, whereas SHP-2 E76A expression even enhanced this compared to cells expressing SHP-2 WT (both $p < 0.05$, n = 5 each 4 fields of view; Figure 1B). Importantly, SHP-2 CS expression

resulted in impaired hypoxic vessel sprouting from aortic segments ex vivo, while SHP-2 E76A expression enhanced this compared to SHP-2 WT ($p < 0.05$, n = 4; Figure 1C). Finally, hypoxia-induced production of the angiogenic factor vascular endothelial growth factor (VEGF) was impaired in SHP-2 CS cells and enhanced in SHP-2 E76A cells compared to SHP-2 WT ($p < 0.05$, n = 3–6; Figure 1D). Having observed that SHP-2 affects angiogenic responses under hypoxia, we further investigated if SHP-2 influences hypoxic HIF-1α accumulation in endothelial cells in vitro. Whereas hypoxic treatment increased HIF-1α protein levels in SHP-2 WT expressing endothelial cells, SHP-2 CS expression decreased and SHP-2 E76A expression enhanced hypoxia-induced HIF-1α levels significantly ($p < 0.05$, n = 6; Figure 1E). In contrast, the expression of a SHP-2 construct with mutations of both its tyrosine phosphorylation sites (Y542/580F, Y2F) did not influence HIF-1α accumulation, proving the observed effects being exclusively dependent on SHP-2 phosphatase activity. Furthermore, promotor binding activity of HIF-1α was reduced in nuclear extracts of SHP-2 CS cells compared to SHP-2 WT cells ($p < 0.05$, n = 3 in duplicates; Figure 1F). Likewise, double transduction of endothelial cells with SHP-2 mutant constructs in combination with a lentiviral HIF1-transcriptional reporter construct (HIF1-TRE-Luc) containing HIF-1 transcriptional response elements (TRE) or control reporter construct lacking the TRE (Control-Luc), respectively, revealed a 2-fold increase in luciferase activity upon hypoxia in SHP-2 WT cells, which was completely inhibited upon SHP-2 CS expression ($p < 0.05$, n = 5; Figure 1G).

SHP-2 Prevents Degradation of HIF-1α under Hypoxic Conditions via Src Kinase Activation

Induction of HIF-1α protein levels can result from increased gene expression or inhibition of its degradation.[25] To elucidate how SHP-2 activity regulates HIF-1α protein levels, we therefore first measured HIF-1α mRNA levels in hypoxic cells expressing the different SHP-2 mutants. Quantitative real-time PCR did not reveal any difference in HIF-1α mRNA expression between SHP-2 WT, CS, and E76A expressing cells upon hypoxic treatment (n = 3 in duplicates; Figure 2A). Live cell detection of HIF-1α mRNA using SmartFlare probes in these cells confirmed this finding (n = 3 in duplicates; Figure 2B). To investigate if SHP-2 instead influences HIF-1α degradation, SHP-2 WT and CS cells were treated with the proteasome inhibitors MG132 and epoxomicin, respectively. Hypoxia increased HIF-1α levels in SHP-2 WT cells ($p < 0.05$, n = 7; Figure 2C) and, as observed in previous experiments (Figure 1E), SHP-2 CS over-expression led to decreased HIF-1α protein accumulation ($p < 0.05$, n = 7). Interestingly, treatment of hypoxic SHP-2 CS cells with MG132 and epoxomicin, respectively, returned the HIF-1α level back to the same level as in hypoxic SHP-2 WT cells treated with proteasome inhibitors ($p < 0.05$, n = 3–4; Figure 2C). Inhibition of PHD activity by desferrioxamine (DFO) in SHP-2 CS expressing cells also returned the decreased HIF-1α protein level back to levels seen in hypoxic SHP-2 WT cells ($p < 0.05$, n = 4; Figure 2D). In addition, a stronger HIF-1α prolyl hydroxylation was detected in SHP-2 CS cells compared to SHP-2 WT cells upon MG132 treatment prior to
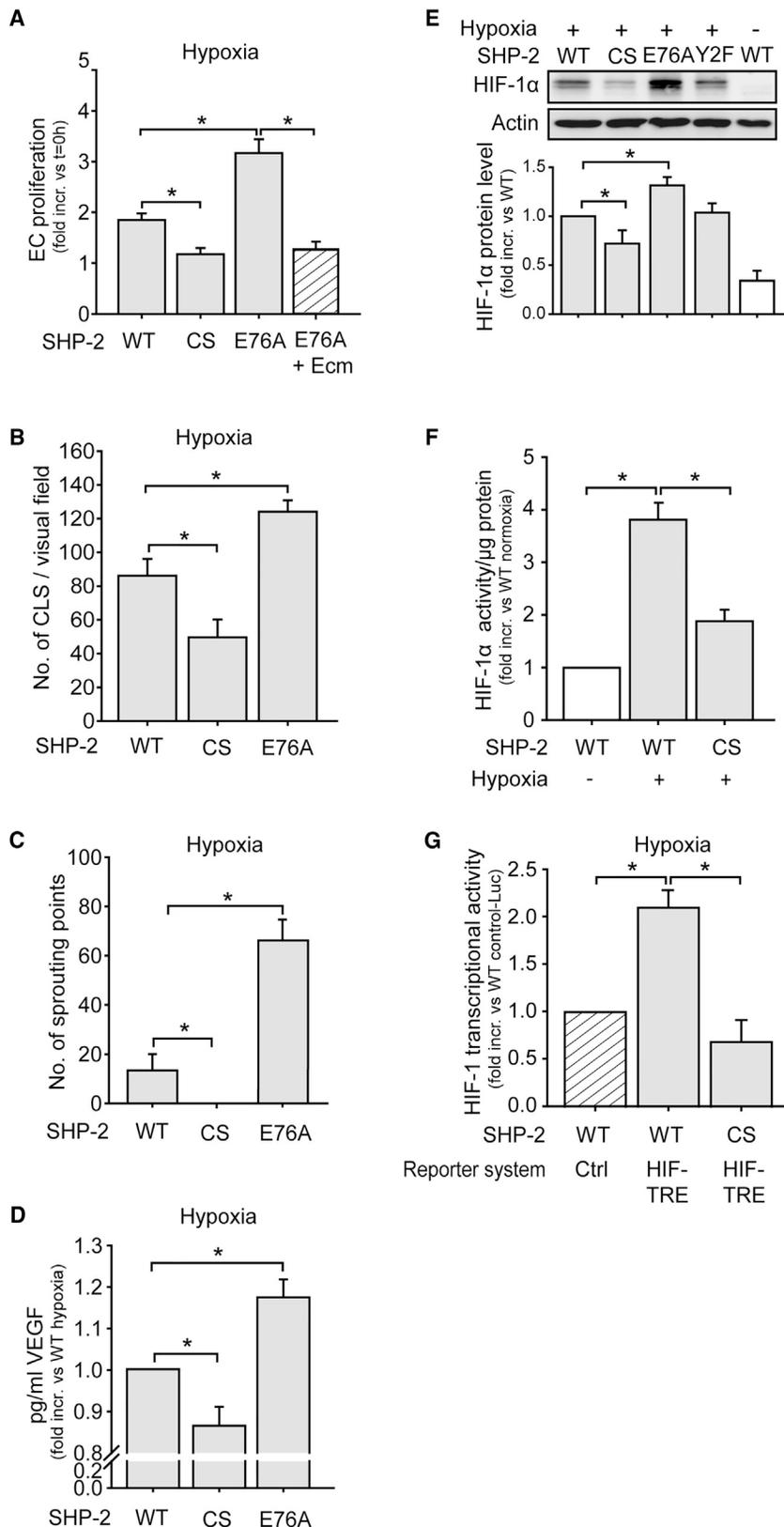
A

B

C

D

E

F

G

Figure 1. SHP-2 Inactivation Inhibits Hypoxia-Induced Angiogenesis and HIF-1α Accumulation and Activity In Vitro

(A) Overexpression of SHP-2 WT, SHP-2 CS (dominant negative mutant), or SHP-2 E76A (constitutively active mutant) was achieved by lentiviral transduction (see Figure S1). Proliferation of endothelial cells expressing the different SHP-2 constructs upon 24 hr hypoxia treatment was assessed by MTT reduction 96 hr post transduction ($*p < 0.05$, n = 5 in triplicates). The enhanced proliferation in SHP-2 E76A cells was inhibited by treatment with 10 ng/mL echinomycin (Ecm) ($p < 0.05$, n = 5 in triplicates). (B) Formation of capillary like structures in Matrigel during hypoxia (24 hr) in SHP-2 WT, CS, and E76A expressing endothelial cells ($*p < 0.05$, n = 5 each, 4 fields of view). The Matrigel assay was performed 96 hr after lentiviral transduction. (C) Vessel sprouting from aortic rings ex vivo expressing SHP-2 WT, CS, or E76A and exposed to hypoxia (24 hr) ($*p < 0.05$, n = 4–5). The isolated vessels were immediately transduced using magnetic targeting of MNP-LV complexes to the vessel wall. At 48 hr later, aortas were cut into rings, embedded in Matrigel, and exposed to hypoxia. (D) Hypoxia-induced (4 hr) VEGF production from SHP-2 WT, CS, or E76A expressing endothelial cells, as assessed by ELISA 96 hr after transduction ($*p < 0.05$, n = 3–6). (E) Analysis of hypoxia-induced (4 hr) HIF-1α accumulation in endothelial cells lentivirally transduced with SHP-2 WT, CS, E76A, or Y2F. The graph shows protein band densities of HIF-1α normalized to actin ($*p < 0.05$, n = 6). (F) HIF-1 DNA binding activity in nuclear extracts of cells expressing SHP-2 WT or CS upon hypoxia (4 hr) was measured using a HIF-1 transcription factor assay kit 96 hr post transduction ($*p < 0.05$, n = 3 in duplicates). (G) HIF-1α activity upon hypoxia (4 hr) in endothelial cells expressing SHP-2 WT or CS was detected 72 hr upon co-transduction of SHP-2 WT or CS in combination with the HIF1-TRE-Luc or Control-Luc reporter construct ($*p < 0.05$, n = 5). All of the quantitative data are represented as mean ± SEM.

A

Hypoxia

HIF-1α mRNA expression (2^{dCt})

SHP-2: WT, CS, E76A

B

Hypoxia

mRNA in GFP+ cells (fold incr. vs WT HIF-1α probe)

SHP-2: WT CS E76A   WT CS E76A

Probe: scramble | HIF-1α

C

Normoxia | Hypoxia

Epoxomicin	-	-	+	-	-	+	-	-	+
MG132	-	+	-	-	+	-	-	+	-
SHP-2	WT	WT	WT	WT	WT	WT	CS	CS	CS

HIF-1α
Actin

HIF-1α protein level (fold incr. vs WT normoxia)

1 2 3 4 5 6 7 8 9

* * * *

D

DFO	-	-	+	-	+
Hypoxia	-	+	+	+	+
SHP-2	WT	WT	WT	CS	CS

HIF-1α
Actin

HIF-1α protein level (fold incr. vs WT normoxia)

n.s
*

E

MG132	+	+	+
Hypoxia	+	+	+
SHP-2	WT	CS	E76A

hydroxy-HIF-1α
Actin

hydroxy-HIF-1α (fold incr. vs WT)

*

F

PP2	-	-	-	+
MG132	-	-	+	+
Hypoxia	-	+	+	+

hydroxy-HIF-1α
Actin

hydroxy-HIF-1α (fold incr. vs hypox+MG)

* * *

G

| Hypoxia | + | + | + |
| SHP-2 | WT | CS | E76A |

phospho-Src
Actin

phospho-Src (fold incr. vs WT)

* *

H

SHP-2 phosphatase activity (fold incr. vs normoxia)
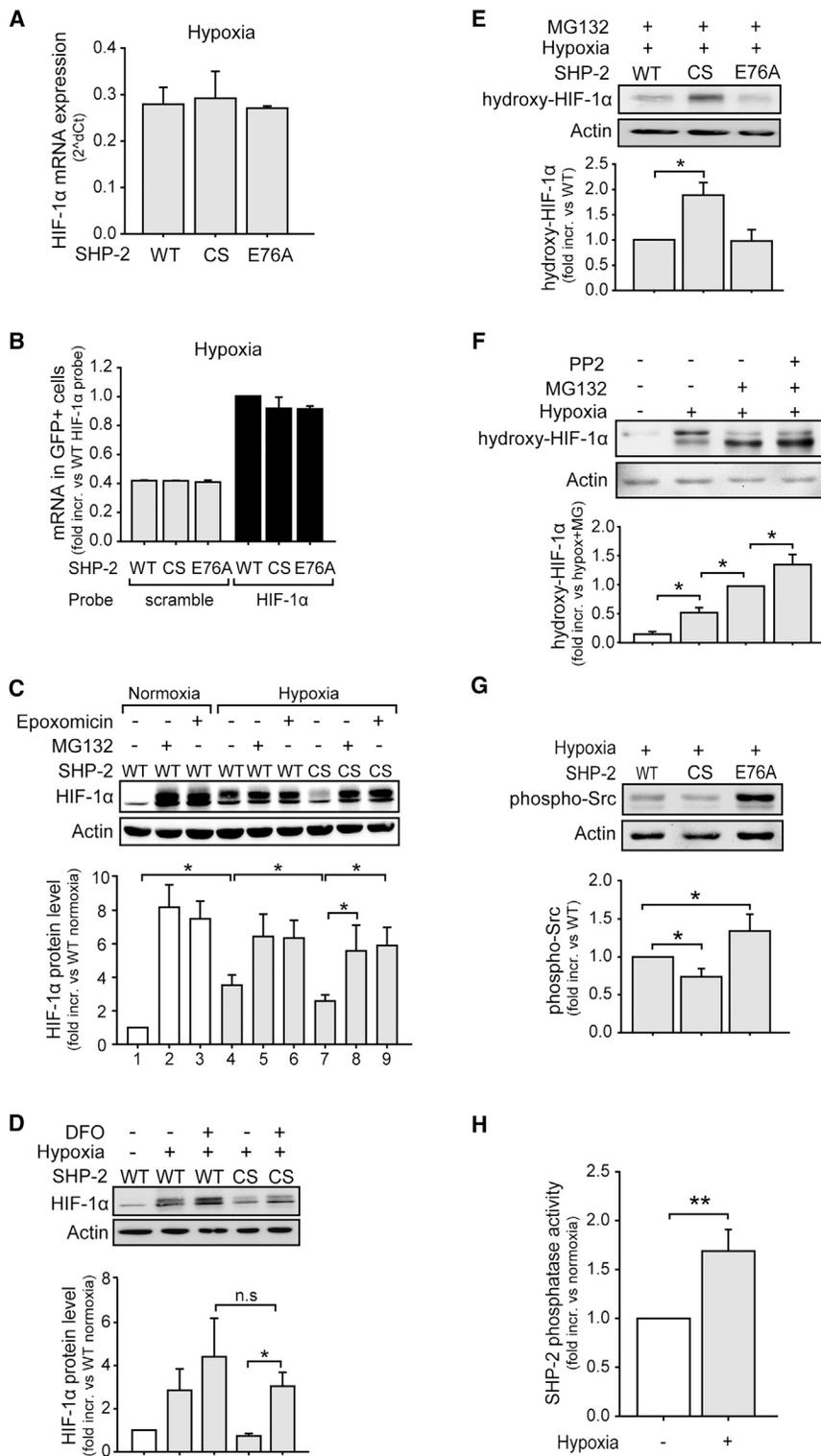
Hypoxia: - +

**

Figure 2. SHP-2 Inhibits HIF-1α Degradation via Activation of the Src Kinase

(A) Hypoxic (4 hr) HIF-1α mRNA expression in cells overexpressing SHP-2 WT, CS, or E76A was assessed by qRT-PCR 96 hr post transduction (n = 3 in duplicates). (B) Live cell HIF-1α mRNA detection in hypoxic (4 hr) cells expressing SHP-2 WT-IRES-eGFP, CS-IRES-eGFP, or E76A-IRES-eGFP, using HIF-1α or scramble (control) SmartFlare probes and flow cytometry 96 hr post transduction (n = 3 in duplicates). The graph shows HIF-1α mRNA in GFP positive cells. (C) MG132 (10 μM) or epoxomicin (1 μM) treatment increased HIF-1α levels in SHP-2 CS expressing cells (lanes 7–9) to the same extent as in SHP-2 WT cells under hypoxia (4 hr) (lanes 4–6) (*p < 0.05, n = 3–7), as assessed by western blot. (D) HIF-1α levels in DFO treated (100 μM) SHP-2 WT or CS expressing cells during hypoxia (4 hr) (*p < 0.05, n = 4). (E) Prolyl-hydroxylated HIF-1α (Pro564) was analyzed in SHP-2 WT, CS, and E76A cells after hypoxia (4 hr) and MG132 (10 μM) treatment by western blot (*p < 0.05, n = 3). The graphs below blots show protein band densities of HIF-1α normalized to actin. (F) Hydroxylation of HIF-1α in endothelial cells during hypoxia (4 hr) upon treatment with Src inhibitor (100 nM PP2) and exposure to MG132 (10 μM) (*p < 0.05, n = 3) was detected using western blot. The graph shows protein band densities of hydroxy-HIF-1α normalized to actin. (G) Hypoxia- (4 hr) induced Src phosphorylation in cells expressing SHP-2 WT, CS, or SHP-2 E76A was analyzed by western blot 96 hr post transduction (*p < 0.05, n = 4–7). The graph shows protein band densities of phospho-Src normalized to actin. See also Figure S2. (H) The influence of hypoxia (4 hr) on SHP-2 phosphatase activity was measured by dephosphorylation of pNPP in SHP-2 precipitates (**p < 0.01, n = 6). All of the quantitative data are represented as mean ± SEM.

vation under hypoxia. First, Src inhibition increased HIF-1α hydroxylation in cells treated with MG132 under hypoxic conditions (p < 0.05, n = 3; Figure 2F), indicating a similar protective effect as SHP-2 from HIF-1α degradation. Next, Src activation was shown to be dependent on SHP-2 activity, as this was reduced in SHP-2 CS expressing cells and enhanced in SHP-2 E76A expressing cells compared to SHP-2 WT expression under hypoxic conditions (p < 0.05, n = 4–7; Figure 2G). A reduction in phosphorylation of other Src kinase family members could also be observed in SHP-2 CS expressing cells compared to SHP-2 WT upon a phospho-Src kinase screen (Figure S2). As we observed that SHP-2 promotes HIF-1α stabilization and activity as well as Src kinase signaling and angiogenesis upon

hypoxia (p < 0.05, n = 3; Figure 2E). As the activation of Src kinase has been shown to rely on SHP-2 activity upon growth factor stimulation,[26] we next investigated if SHP-2, in addition, influences Src acti-

hypoxia, we next measured endogenous SHP-2 phosphatase activity upon hypoxia. As seen in Figure 2H, hypoxia significantly increased SHP-2 activity (p < 0.01, n = 6).

Magnetic Targeting of MNP-LV Complexes Accomplishes Simultaneous but Differential Gene Expression at Defined Sites in the Dorsal Skin of Mice

As we aimed at investigating the role of SHP-2 in HIF-1α dependent angiogenesis, we first assessed vessel outgrowth in an in vivo wound healing model over a period of time using the mouse dorsal skinfold chamber. This was enabled by intravenous injection of FITC-Dextran followed by intravital fluorescent microscopy ($p < 0.05$ versus first observation time point, n = 3 animals; Figure 3A). In order to later study the effect of SHP-2 phosphatase activity in this in vivo wound healing model to elucidate its potential as a therapeutic target, we established a localized transduction technique to the dorsal skin by using lentiviral particles associated to MNP and achieved their targeting to the dorsal skin by exposure to a magnetic field. As seen in Figure 3B, magnetic targeting of a luciferase expressing lentivirus associated to MNP resulted in local luciferase expression in the targeted dorsal skin. In fact, no transgene expression was detected at any other site, demonstrating the local specificity of the technique (Figure S3). Moreover, no reporter gene expression was observed in the absence of a magnetic field (Figure 3B). To elucidate if magnetic targeting of MNP-LV complexes and the resulting gene expression influences the wound healing response per se, MNP associated to SHP-2 WT expressing lentivirus was targeted to wounds of the dorsal skin and compared to non-treated wounds. As seen in Figure 3C, no difference between the two groups was observed (n = 3–7 animals). Importantly, we were able to achieve independent local transduction of up to three areas within the same dorsal skinfold chamber using this technique, as seen by the differential gene expression strength, which correlated well with the amount of applied lentiviral particles (Figure 3D). Importantly, there was no contamination between the different wounds, as only the wound exposed to MNP-LV complexes in combination with a MF expressed the transgene, although other wounds treated with only sodium chloride in the same dorsal skinfold chamber were exposed to the MF (Figure 3E). Furthermore, magnetic targeting of MNP and LV expressing SHP-2 WT and td Tomato via an IRES sequence showed that gene expression could be directed with high precision to the wound area (Figure 3F; n = 3).

Genetic Modulation of SHP-2 Phosphatase Activity by Magnetic LV-MNP Targeting Controls HIF-1α Dependent Wound Healing Angiogenesis In Vivo

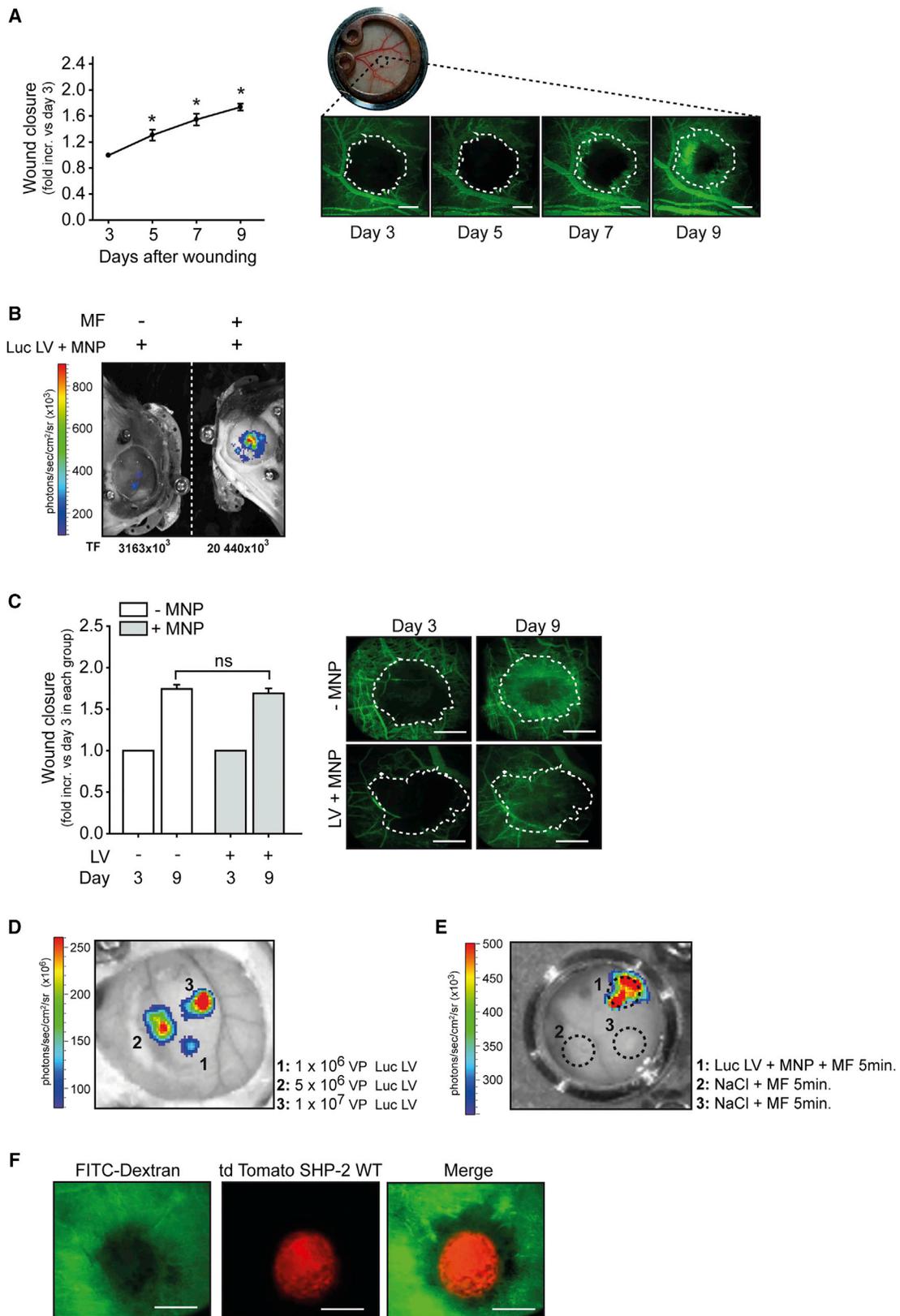Having observed that SHP-2 affects hypoxic HIF-1α accumulation and activity in vitro, we next investigated if SHP-2 has the same effect in vivo. In order to precisely visualize the induction of HIF-1 transcriptional activity in wounds in vivo, the lentiviral HIF1-transcriptional reporter construct HIF1-TRE-Luc or control reporter construct Control-Luc was delivered to individual wounds in the dorsal skinfold chamber by local magnetic targeting of MNP-LV complexes (Figure 4). Only weak bioluminescence signals could be detected in HIF1-TRE-Luc transduced intact areas or wounds transduced with Control-Luc (n = 8 animals; Figure 5A). In contrast, high and local HIF-1 activity was detected within the wound area, as indicated by HIF-1 dependent luciferase expression ($p < 0.05$, n = 8 animals; Figure 5A), verifying the relevance of HIF-1α for wound healing. Further-

more, overexpression of SHP-2 CS in wounds, using magnetic targeted transduction, impaired vessel outgrowth and thus wound healing compared to SHP-2 WT overexpression ($p < 0.05$, n = 5 animals; Figures 4 and 5B). In contrast, overexpression of SHP-2 E76A in the wound significantly accelerated vessel outgrowth and thus wound closure ($p < 0.05$, n = 5 animals; Figure 5B). To verify the influence of SHP-2 on HIF-1α activity in vivo, three individual wounds within one dorsal skinfold chamber were simultaneously co-transduced with the different lentiviral SHP-2 mutants and the HIF1-TRE-Luc reporter or Control-Luc reporter construct using MNP mediated targeting, respectively (Figure 4). While no luciferase expression could be detected in wounds co-transduced with the different SHP-2 constructs and the Control-Luc reporter construct lacking the HIF-1 TRE sequence, wounds co-expressing SHP-2 WT/HIF1-TRE-Luc showed strong luciferase activity resulting from endogenous HIF-1α accumulation in the wound (Figure 5C). However, in wounds with localized SHP-2 CS/HIF1-TRE-Luc expression, only weak luciferase activity was detected indicating diminished HIF-1α accumulation ($p < 0.05$, n = 4; Figure 5C). In contrast, SHP-2 E76A expression further enhanced HIF-1α transcriptional activity in hypoxic wounds in vivo compared to SHP-2 WT ($p < 0.05$, n = 4 animals; Figure 5C). Moreover, whereas the mRNA of the HIF-1α target genes VEGF-A, PDGF-B, and MMP-2 were increased in wounds compared to healthy surrounding tissue ($p < 0.05$, n = 5; Figure 5D), expression of SHP-2 CS in wounds reduced mRNA expression of these genes compared to wounds expressing SHP-2 WT ($p < 0.05$, n = 3–5; Figure 5D).

DISCUSSION

Hypoxia induces vascularization by stabilizing HIF-1α leading to transcription of angiogenic factors. Hypoxia dependent vessel formation is an important feature in several medical conditions, such as tumor growth, diabetic retinopathy, and ischemia, and efforts have been made to reverse the disease phenotype by targeting HIF-1α.[13] In this study, we demonstrate that the tyrosine phosphatase activity of SHP-2 positively influences hypoxia dependent angiogenesis in vitro as well as in vivo by supporting stabilization and accumulation of HIF-1α. Thus, we identify SHP-2 as a potential therapeutic target for modulating HIF-1α dependent vascularization. By introducing the expression of SHP-2 mutants in wounds using magnetic targeting of MNP-LV complexes, wound healing angiogenesis can be controlled site-specifically in vivo.

Our data reveal that SHP-2 is essential for the angiogenic response of endothelial cells under hypoxic conditions, as well as for wound healing angiogenesis in vivo, where hypoxia is the major driving factor.[27] This is in accordance with the impaired vessel formation of the chicken chorioallantoic membrane observed after SHP-2 pharmacological inhibition from an earlier study by us,[22] further emphasizing a promoting role of SHP-2 in vessel growth. In fact, here, we found SHP-2 phosphatase activity to affect hypoxic angiogenesis by increasing HIF-1α protein levels, HIF-1α DNA binding activity, as well as HIF-1α transcriptional activity, resulting in production of angiogenic factors, such as VEGF-A, PDGF-B, and MMP-2. We demonstrate that SHP-2 promotes HIF-1α accumulation by

A

B

C

D

1: 1 x 10^6 VP Luc LV
2: 5 x 10^6 VP Luc LV
3: 1 x 10^7 VP Luc LV

E

1: Luc LV + MNP + MF 5min.
2: NaCl + MF 5min.
3: NaCl + MF 5min.

F

(legend on next page)

inhibiting its degradation via a Src kinase dependent mechanism, as proteasome as well as PHD inhibition rescued the low HIF-1α protein levels in SHP-2 CS expressing cells. The detection of stronger HIF-1α prolyl hydroxylation in these cells confirms these findings. Of note, the influence of SHP-2 on HIF-1α accumulation and activity was shown to indeed be physiologically relevant, as modulation of SHP-2 activity in wounds in mice regulated local HIF-1α activity and consequentially the expression of HIF-1α target genes in these wounds, thus controlling the wound healing response. Most excitingly, by using our magnetic gene targeting technique, we were able to induce expression of a desired gene with high precision to a specific site, the wound, and did thereby not only confirm the SHP-2 dependent mechanism observed in vitro in an equivalent and physiologically relevant in vivo set up, but also demonstrate the therapeutic potential of SHP-2 for angiogenesis. Furthermore, the observation that SHP-2 activity is increased under hypoxic conditions strongly arguments for a physiologically relevant and promoting role of SHP-2 in HIF-1α dependent angiogenesis. Thus, our findings uncover a so far unrecognized, but significant, role of SHP-2 for hypoxic angiogenesis determining HIF-1α accumulation and activity.

For patho-physiological conditions with impaired wound healing and decreased HIF-1α expression, such as diabetic wounds,[28,29] as well as for conditions with enhanced vascularization, such as tumors expressing high levels of HIF-1α,[13] controlling SHP-2 activity may improve disease. Indeed, this was demonstrated by our in vivo technique using magnetic targeting of MNP-LV complexes to individual wounds of the mouse dorsal skinfold chamber. This elegantly did not only allow direct measurement of HIF-1α activity in the wound by transduction of a HIF1-TRE reporter construct, but additionally empowered simultaneous expression of different SHP-2 gene constructs inducing enhanced as well as decreased HIF-1α expression and wound healing responses, respectively, in defined regions of the same tissue in one animal. Thus, HIF-1α expression in wounds in vivo can indeed be controlled by genetic modulation of SHP-2 activity.

Therefore, this technique may be of great therapeutic interest, as it enables the selective interference with angiogenic processes in defined areas exclusively. The ability to design magnetic fields with powerful enough field gradients to reach distant and deeper situated sites will determine the actual potential and the extent of translation of this technique into the clinic.

In summary, we did not only achieve desired differential gene expression at defined sites of the same tissue by using magnetic targeting of MNP and lentiviral particles, but we also unveil a decisive role of SHP-2 in promoting the stabilization and activation of HIF-1α upon hypoxia through Src signaling, thereby having an essential impact on hypoxia and HIF-1α dependent angiogenesis in vitro and in vivo. Thus, modulation of SHP-2 activity and so HIF-1α accumulation in diseased areas by magnetic targeting may be a powerful tool to improve patho-physiological conditions involving vascularization.

MATERIALS AND METHODS
Antibodies and Chemicals
Hydroxy-HIF-1α (Pro564) (#3434), phospho-Src (Y416) (#2101), myc-tag (#2276), and β-Actin (13E5) (#4970) antibodies were from Cell Signaling Technology. HIF-1α clone H1α67 (#MAB5382), HIF-1α clone EP1215Y (#04-1006), anti-mouse (#401253), and rabbit (#401353) horseradish peroxidase-conjugated secondary antibodies were from Merck Millipore. Epoxomicin and PP2 were from Calbiochem. Luciferin was purchased from Promega. All other chemicals were from Sigma-Aldrich.

Human Microvascular Endothelial Cell Culture
Human microvascular endothelial cell (HMEC) were cultivated as previously described.[30]

Lentiviral Constructs and Transductions
Plasmid vectors of WT SHP-2 and the catalytically inactive mutant SHP-2 CS (Cys459 to Ser459) were kind gifts from the Bennett

Figure 3. Magnetic Mediated MNP-LV Gene Delivery Allows for Gene Expression in Wounds in the Dorsal Skin of Mice
(A) Time course of wound closure of the subcutaneous layer in the mouse dorsal skinfold chamber model (*p < 0.05 versus time point of first measurement, n = 3 animals). The dorsal skin of mice was wounded using a hot probe and wound size was detected by FITC-Dextran injection and fluorescent intravital microscopy at denoted time points. The representative intravital microscopy images of wounds after FITC-Dextran injection for visualization of vessel growth into wounds are shown (right). The white dotted line marks initial wound area as measured on day 3 (first measurement). The bar in photos represents 500 μm. (B) Application of luciferase expressing lentiviral particles (Luc LV) associated to MNP resulted in local luciferase expression only when a magnetic field (MF) was applied to the dorsal skinfold chamber (right). The total photon flux (TF) (photons/sec) was determined using region of interest (ROI) measurements. The bioluminescence measurements by intraperitoneal luciferin injection were performed 6 days post transduction. See also Figure S3. (C) Comparison in wound healing response between non-treated (no MNP-LV; white bars) wounds and wounds with magnetic targeting of MNP associated to lentivirus expressing SHP-2 WT (gray bars). The fluorescent intravital microscopy was performed 3 and 9 days post transduction, respectively, by injection of FITC-Dextran. The wound closure at day 9 was normalized to day 3 of the respective wound. ns: not significant, n = 3–7. The representative intravital microscopy images of wounds after FITC-Dextran injection are shown (right). The white dotted line marks the initial wound area as measured on day 3 (first measurement). The bar in photos represents 500 μm. (D) Magnetic targeting of MNP associated to different lentiviral particle amounts (VP) of luciferase expressing lentivirus to defined areas of the same dorsal skinfold chamber correlates with the respective different luciferase expression strength. The bioluminescence measurements by intraperitoneal luciferin injection were performed 6 days post transduction. (1) application of 1 × 10^6 VP; (2) application of 5 × 10^6 VP; and (3) application of 1 × 10^7 VP. (E) Magnetic targeting of MNP associated to a luciferase expressing lentivirus to a wound induces expression of the transgene 6 days after transduction, whereas no expression was detected in other wounds of the same dorsal skinfold chamber treated with only sodium chloride solution and exposed to the magnetic field (MF). The dotted circles mark the wounds. (F) Intravital microscopy images of wounds after FITC-Dextran injection (green) and magnetic targeting of MNP associated to lentivirus expressing SHP-2 WT and td Tomato via an IRES element showing transgene expression in the wound (red) 6 days after transduction. The bar in photos represents 500 μm. All of the quantitative data are represented as mean ± SEM.
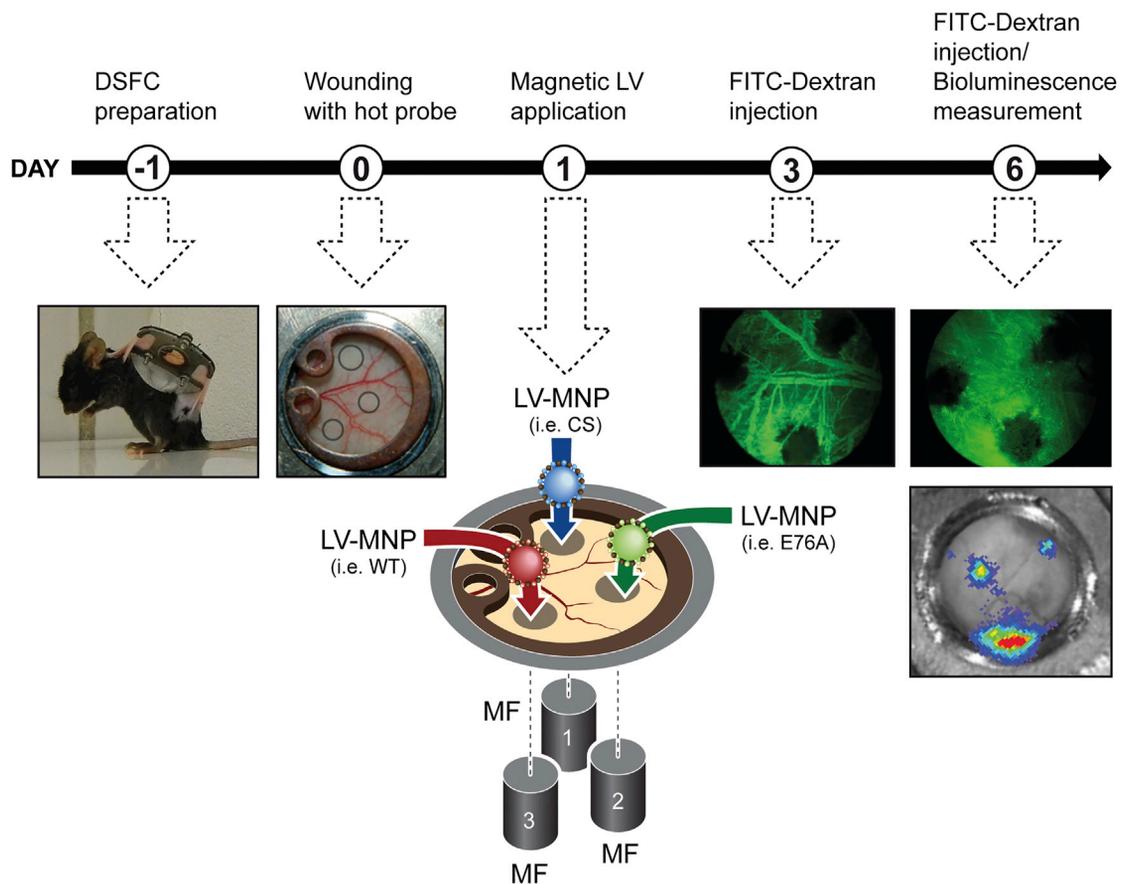
Figure 4. Scheme of Site-Specific Expression of SHP-2 Mutants and HIF1-TRE-Luc in Wounds in the Dorsal Skinfold Chamber in Mice

Day 1: Preparation of the dorsal skinfold chamber on C57BL/6J mice. Day 0: Up to three wounds were induced within the observation window using a heated wire. Day 1: Lentiviral vectors carrying expression vectors for SHP-2 mutants (WT, CS, and E76A), HIF1-TRE-Luc, or Control-Luc, respectively, were associated to magnetic nano-particles[10] and individually applied to the wounds under magnetic field exposure. Day 3: First measurement of wound size and vessel growth within the wound by intravenous injection of FITC-Dextran and intravital microscopy. Day 6: Measurement of wound size and vessel growth within the wound by intravenous injection of FITC-Dextran and intravital microscopy (SHP-2 WT, CS, and E76A) or detection of bioluminescence in wounds (HIF1-TRE-Luc and Control-Luc).

laboratory,[31] the tyrosine phosphorylation sites SHP-2 mutant (Y2F), used to analyze involvement of SHP-2 phosphorylation, was kindly provided by Professor F. Schaper at Magdeburg University, Germany. Mutation of Glu76 to Ala76 to generate the constitutively active SHP-2 E76A was produced using the SHP-2 WT vector and the QuikChange II XL Site-Directed Mutagenesis Kit (Agilent) according to the manufacturers' instructions. The different cDNAs were subcloned into a self-inactivating RRL-lentiviral backbone (pcDNA3) under control of a CMV-promoter with IRES-GFP or IRES-td Tomato co-expression. The HIF1-TRE-Luc lentiviral plasmid was obtained from System Biosciences (pGreenFire1-HIF1). The control lentiviral plasmid (Ctrl-Luc) was generated by excision of the TRE-sequence from the HIF-TRE-Luc lentiviral plasmid using EcoRI and SpeI, followed by generation of blunt ends and fill-in using Klenow Large DNA polymerase I and religation. Sequences were verified by DNA sequencing. Lentiviral particles were produced as previously described.[11] The biological titer was determined by flow cytometry of transduced HEK293T cells as described elsewhere.[11] Lentiviral

transduction of HMECs was performed using a multiplicity of infection (MOI) of 5. Lentiviral particles were diluted in Hank's solution and applied onto subconfluent HMEC. After incubation for 4–6 hr at 37°C, culture medium was added and medium was changed the next day. Cells were left 72 hr before assaying.

Hypoxia Treatment

HMECs were exposed to hypoxia (pO_2 8 ± 2 mmHg equivalent to a O_2 concentration of 1 ± 0.2%) for indicated times in a hypoxia chamber (Cell Systems) as previously described.[32]

Quantitative Real-Time PCR

Total RNA from HMEC was isolated and quantitative reverse-transcriptase PCR (qRT-PCR) of HIF-1α RNA was performed as described before.[32] To isolate total RNA from mouse tissue, wound or healthy areas were excised and mechanically ground in RNA lysis buffer by using Precellys ceramic beads (PEQLAB). qRT-PCR was performed as described before[32] using the following primers
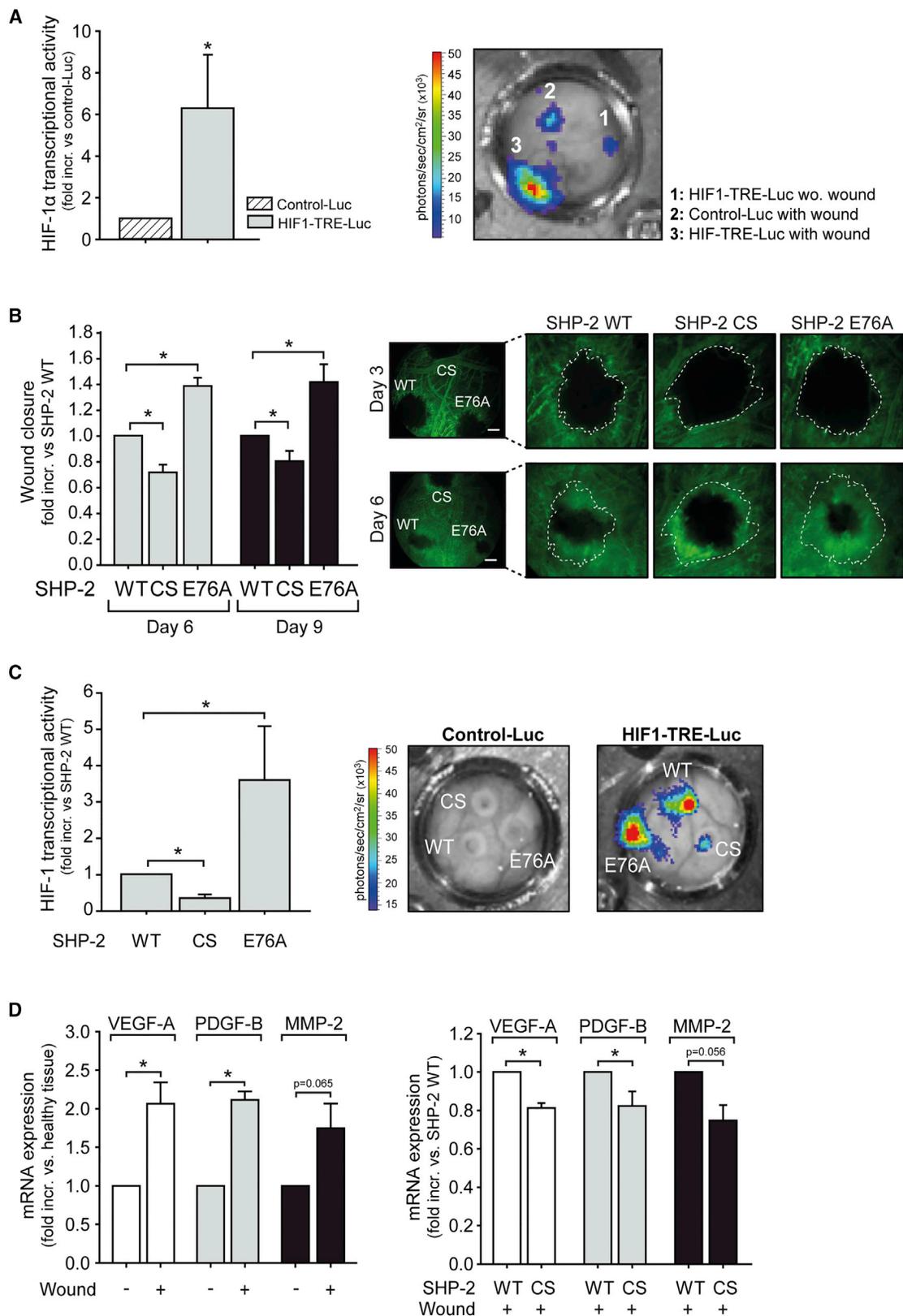
(legend on next page)

(Metabion): *VEGF* fw: TATTCAGCGGACTCACCAGC and rv: AA
CCAACCTCCTCAAACCGT; *MMP2* fw: TCTGCGATGAGCTTAG
GGAAAC and rv: GACATACATCTTTGCAGGAGACAAG *PDGF-B*
fw: AAGTGTGAGACAATAGTGACCCC and rv: CATGGGTGTGC
TTAAACTTTCG; and *Ribosomal protein S18* fw: GTTCCAGCA
CATTTTGCGAGT and rv: GAGTTCTCCAGCCCTCTTGG.

Live Cell HIF-1α RNA Detection with SmartFlare Probes

Detection and quantification of HIF-1α mRNA in live cells expressing
different SHP-2 constructs coupled to an IRES-GFP cassette were
performed using HIF-1α and scrambled SmartFlare probes and
flow cytometry according to the supplier's protocol (Invitrogen). In
detail, cells were transduced with SHP-2 WT, CS, or E76A expressing
lentivirus and seeded on to 96-well plates. 72 hr later, cells were incu-
bated with the HIF-1α probe or a scrambled probe (SF-102) as control
2 hr prior to hypoxia treatment to allow for efficient uptake of the
probes. After 4 hr of hypoxia, cells were immediately analyzed
by flow cytometry. Detection of SmartFlare probes was only
performed in cells positive for GFP (SHP-2 WT, CS, and E76A ex-
pressing cells) as determined by flow cytometry. A fluorescent probe
(SF-137) was used to control for SmartFlare uptake.

Detection of VEGF Production

VEGF-A concentrations in cell supernatants were detected by Quan-
tikine ELISA (#DVE00, R&D Systems) according to the supplier's
protocol.

Immunoblotting

Lysates were prepared and subjected to SDS-PAGE following western
blotting as described elsewhere.[33] Protein band intensities were
measured using the Hokawo software (Hamamatsu).

Wound Healing Assay In Vivo and Lentiviral Magnetic Targeting

Animal studies were conducted in accordance with the German ani-
mal protection law and approved by the district government of upper
Bavaria (Regierung von Oberbayern, approval reference number
AZ55.2-1-54-2532-172-13). The investigation conforms to the *Guide
for the Care and Use of Laboratory Animals* published by the US
National Institutes of Health (NIH Publication No. 85-23, revised
1996). Mice (C57BL/6J; Charles River) were anesthetized (5 mg/kg

midazolam, 0.5 mg/kg medetomidin, and 0.05 mg/kg fentanyl) and
the dorsal skinfold chamber was implanted as described elsewhere.[34]
Up to three wounds were induced within the observation window of
one DSFC 24 hr after implantation. In detail, a heated wire (1 mm
diameter) was applied at an avascular area of the internal skin side
for 5 s. The resulting wound (2 mm diameter) was moistened
following induction of the next wound. Distinct gene expression
within the different wounds was achieved by MNP assisted lentiviral
transduction 24 hr after wound induction. The lentiviral vectors
(1.5×10^7 VP HIF1-TRE-Luc, control-Luc, or SHP-2 WT/CS/
E76A) were incubated separately or in the indicated combinations
with 1 μg SO-Mag MNPs[35] for 10 min to allow for association. To
achieve individual transductions, a cylindrical permanent magnet
(diameter 3 mm, height 15 mm; 1,120 mT) was placed under the
respective wound and lentivirus-MNP-complexes were applied on
top. The magnetic field was applied for 5 min before the next wound
was transduced successively. After removing the magnetic field, the
dorsal skin was washed with 0.9% sodium chloride solution and the
observation window was tightly closed with a coverslip. For measure-
ment of wound areas, mice were restrained in plexiglass tubes and
20 μL FITC dextran (150 kDa, 5% in NaCl) were injected intrave-
nously via the tail vein. Images were taken using an intravital fluores-
cence microscope (Zeiss) and avascular wound areas were measured
using the AxioVision software (Zeiss). Bioluminescence imaging was
performed using an IVIS imaging system (PerkinElmer) 6 days after
magnetic targeting by intraperitoneal injection of 100 μL (3 mg/mL in
0.9% NaCl) Luciferin.

HIF-1α DNA Binding Activity

Specific HRE binding activity of HIF-1α was measured in nuclear ex-
tracts of HMECs using the Transcription Factor Assay Kit (#KA1321)
from Abnova, following manufacturer's instructions.

Aortic Ring Sprouting Assay

Aortas were isolated from euthanized mice as previously described.[22]
Whole aortas were transduced with SHP-2 lentiviral particles using
the magnetofection technique.[10] In detail, lentiviral particles were
incubated with PEI-Mag2 MNP (300 fg/VP) in Hanks balanced salt
solution for 20 min at room temperature. Aortas were cannulized
at both ends, flushed with lentiviral-MNP complexes, and placed

Figure 5. SHP-2 Activity Is Necessary for HIF-1α Dependent Angiogenesis In Vivo
(A) HIF-1α expression and activity in wounds were detected by local expression of a lentiviral HIF-1 transcriptional luciferase reporter construct (HIF1-TRE-Luc) in the wound
and compared to transduction of a control luciferase reporter construct missing the HIF1-TRE (Control-Luc) (*p < 0.05, n = 8 animals). The representative bioluminescence
image of luciferase activity in wounds of the dorsal skinfold chamber after magnetic assisted transduction with HIF1-TRE-Luc and Control-Luc, respectively, is shown (right).
1: HIF1-TRE-Luc transduction without wounding; 2: Control-Luc transduction of wound; and 3: HIF1-TRE-Luc transduction of wound. (B) Influence of SHP-2 WT, CS, and
E76A expression in the wound area on vessel growth and wound closure (*p < 0.05, n = 5 animals). The expression of SHP-2 constructs was achieved using magnetic
targeting of MNP-LV complexes. The wound sizes were normalized to respective wounds from day 3. The representative intravital microscopy images taken after intravenous
injection of FITC-Dextran at day 3 and 6 after wounding showing the vessel growth into the wounds of one animal simultaneously expressing different SHP-2 constructs in
separate wounds are shown (right). The white dotted lines mark the initial wound area of the respective wound as measured on day 3. The bar in photos represents 500 μm.
(C) Luciferase expression and thus HIF-1α transcriptional activity 6 days post co-transduction of HIF1-TRE-Luc and different SHP-2 mutant constructs in wounds in the
mouse dorsal skinfold chamber by magnetic targeting of MNP-LV complexes (*p < 0.05, n = 4 animals). The representative bioluminescence images next to the graph show
wounds transduced with control-Luc (left) or HIF1-TRE-Luc (right) vectors in combination with SHP-2 WT and mutant constructs, respectively. (D) mRNA expression of
VEGF-A, PDGF-B, and MMP-2 was measured in wounds and healthy tissue of the mouse dorsal skin by qRT-PCR (left graph) (*p < 0.05, n = 5), as well as in wounds
expressing SHP-2 WT or SHP-2 CS (right graph) (*p < 0.05, n = 3–5). All of the quantitative data are represented as mean ± SEM.

on top of a permanent magnet for 30 min in medium containing 10% FCS and 1% Pen-Strep at 37°C in a humidified incubator with 5% CO_2. Aortas were then left for 48 hr to allow for SHP-2 mutant gene expression, cut into rings, and embedded in growth factor reduced Matrigel (BD Biosciences) followed by exposure to hypoxia for 24 hr to allow for HIF-1α expression. At 72 hr later, images were taken with a Zeiss Axiovert 200 M microscope and the sprouting evaluated as previously described.[22]

Proliferation Assay
Proliferation was measured after 24 hr of hypoxia exposure using the MTT assay as previously described.[22]

SHP-2 Phosphatase Activity Assay
300 μg of total protein was used for precipitation of SHP-2 with a mouse anti-human SHP-2 (B-1) antibody. SHP-2-antibody complexes were precipitated using μMACS Protein G MicroBeads and μMACS separation columns from Miltenyi Biotec. Precipitated SHP-2 was washed with phosphatase buffer (24 mM HEPES, 120 mM NaCl, and pH 7.4) and phosphatase activity was detected by incubation in phosphatase buffer containing 10 mM of the chromogenic substrate p-nitrophenyl phosphate (pNPP) for 1 hr at 37°C in the dark. Supernatants from the precipitations were collected and the extinction was measured at 405 nm (SpectraFluor, Tecan).

Statistical Analysis
Data are presented as means ± SEM. Statistical analyses were performed with Sigma Plot 10.0. For comparisons between two groups of normal distributed data the student's t test was used. For multiple comparisons the one-way ANOVA was performed. Differences were considered significant at an error probability level of $p < 0.05$.

SUPPLEMENTAL INFORMATION
Supplemental Information includes Supplemental Materials and Methods and three figures and can be found with this article online at http://dx.doi.org/10.1016/j.ymthe.2017.04.007.

AUTHOR CONTRIBUTIONS
Y.H. planned, performed, and analyzed most experiments; K.P. performed experiments and revised the manuscript; M.A. performed some in vivo experiments; C.P. helped with bioluminescence measurements and revised the manuscript; O.M. produced the MNP; J.P., P.K., F.K., and U.P. revised the manuscript for intellectual content; A.P. produced lentiviral particles and proof read the manuscript; M.W. and A.R. performed qRT-PCRs; and H.M. designed the study, analyzed the data, performed several experiments, and wrote the manuscript.

CONFLICTS OF INTEREST
The authors have declared that no conflicts of interest exist.

ACKNOWLEDGMENTS

REFERENCES

1. Ylä-Herttuala, S. (2013). Cardiovascular gene therapy with vascular endothelial growth factors. Gene 525, 217–219.

2. Malecki, M., Kolsut, P., and Proczka, R. (2005). Angiogenic and antiangiogenic gene therapy. Gene Ther. 12 (Suppl 1), S159–S169.

3. Liu, P.Y., Liu, K., Wang, X.T., Badiavas, E., Rieger-Christ, K.M., Tang, J.B., and Summerhayes, I.C. (2005). Efficacy of combination gene therapy with multiple growth factor cDNAs to enhance skin flap survival in a rat model. DNA Cell Biol. 24, 751–757.

4. Persano, L., Crescenzi, M., and Indraccolo, S. (2007). Anti-angiogenic gene therapy of cancer: current status and future prospects. Mol. Aspects Med. 28, 87–114.

5. Agarwal, A., Ingham, S.A., Harkins, K.A., Do, D.V., and Nguyen, Q.D. (2016). The role of pharmacogenetics and advances in gene therapy in the treatment of diabetic retinopathy. Pharmacogenomics 17, 309–320.

6. Plank, C., Schillinger, U., Scherer, F., Bergemann, C., Rémy, J.S., Krötz, F., Anton, M., Lausier, J., and Rosenecker, J. (2003). The magnetofection method: using magnetic force to enhance gene delivery. Biol. Chem. 384, 737–747.

7. Scherer, F., Anton, M., Schillinger, U., Henke, J., Bergemann, C., Krüger, A., Gänsbacher, B., and Plank, C. (2002). Magnetofection: enhancing and targeting gene delivery by magnetic force in vitro and in vivo. Gene Ther. 9, 102–109.

8. Mykhaylyk, O., Zelphati, O., Rosenecker, J., and Plank, C. (2008). siRNA delivery by magnetofection. Curr. Opin. Mol. Ther. 10, 493–505.

9. Krötz, F., Sohn, H.Y., Gloe, T., Plank, C., and Pohl, U. (2003). Magnetofection potentiates gene delivery to cultured endothelial cells. J. Vasc. Res. 40, 425–434.

10. Trueck, C., Zimmermann, K., Mykhaylyk, O., Anton, M., Vosen, S., Wenzel, D., Fleischmann, B.K., and Pfeifer, A. (2012). Optimization of magnetic nanoparticle-assisted lentiviral gene transfer. Pharm. Res. 29, 1255–1269.

11. Hofmann, A., Wenzel, D., Becher, U.M., Freitag, D.F., Klein, A.M., Eberbeck, D., Schulte, M., Zimmermann, K., Bergemann, C., Gleich, B., et al. (2009). Combined targeting of lentiviral vectors and positioning of transduced cells by magnetic nanoparticles. Proc. Natl. Acad. Sci. USA 106, 44–49.

12. Mannell, H., Pircher, J., Räthel, T., Schilberg, K., Zimmermann, K., Pfeifer, A., Mykhaylyk, O., Gleich, B., Pohl, U., and Krötz, F. (2012). Targeted endothelial gene delivery by ultrasonic destruction of magnetic microbubbles carrying lentiviral vectors. Pharm. Res. 29, 1282–1294.

13. Rey, S., and Semenza, G.L. (2010). Hypoxia-inducible factor-1-dependent mechanisms of vascularization and vascular remodelling. Cardiovasc. Res. 86, 236–242.

14. Walshe, T.E., and D'Amore, P.A. (2008). The role of hypoxia in vascular injury and repair. Annu. Rev. Pathol. 3, 615–643.

15. Bilton, R.L., and Booker, G.W. (2003). The subtle side to hypoxia inducible factor (HIFalpha) regulation. Eur. J. Biochem. 270, 791–798.

16. Botusan, I.R., Sunkari, V.G., Savu, O., Catrina, A.I., Grünler, J., Lindberg, S., Pereira, T., Ylä-Herttuala, S., Poellinger, L., Brismar, K., and Catrina, S.B. (2008). Stabilization of HIF-1alpha is critical to improve wound healing in diabetic mice. Proc. Natl. Acad. Sci. USA 105, 19426–19431.

17. Mace, K.A., Yu, D.H., Paydar, K.Z., Boudreau, N., and Young, D.M. (2007). Sustained expression of Hif-1α in the diabetic environment promotes angiogenesis and cutaneous wound repair. Wound Repair Regen. 15, 636–645.

18. Sarkar, K., Fox-Talbot, K., Steenbergen, C., Bosch-Marcé, M., and Semenza, G.L. (2009). Adenoviral transfer of HIF-1alpha enhances vascular responses to critical limb ischemia in diabetic mice. Proc. Natl. Acad. Sci. USA 106, 18769–18774.

19. Lee, K., Zhang, H., Qian, D.Z., Rey, S., Liu, J.O., and Semenza, G.L. (2009). Acriflavine inhibits HIF-1 dimerization, tumor growth, and vascularization. Proc. Natl. Acad. Sci. USA 106, 17910–17915.

20. Zhang, H., Qian, D.Z., Tan, Y.S., Lee, K., Gao, P., Ren, Y.R., Rey, S., Hammers, H., Chang, D., Pili, R., et al. (2008). Digoxin and other cardiac glycosides inhibit HIF-1alpha synthesis and block tumor growth. Proc. Natl. Acad. Sci. USA 105, 19579–19586.

21. DeNiro, M., Al-Halafi, A., Al-Mohanna, F.H., Alsmadi, O., and Al-Mohanna, F.A. (2010). Pleiotropic effects of YC-1 selectively inhibit pathological retinal

neovascularization and promote physiological revascularization in a mouse model of oxygen-induced retinopathy. Mol. Pharmacol. *77*, 348–367.

22. Mannell, H., Hellwig, N., Gloe, T., Plank, C., Sohn, H.Y., Groesser, L., Walzog, B., Pohl, U., and Krotz, F. (2008). Inhibition of the tyrosine phosphatase SHP-2 suppresses angiogenesis in vitro and in vivo. J. Vasc. Res. *45*, 153–163.

23. Saxton, T.M., Henkemeyer, M., Gasca, S., Shen, R., Rossi, D.J., Shalaby, F., Feng, G.S., and Pawson, T. (1997). Abnormal mesoderm patterning in mouse embryos mutant for the SH2 tyrosine phosphatase Shp-2. EMBO J. *16*, 2352–2364.

24. Kong, D., Park, E.J., Stephen, A.G., Calvani, M., Cardellina, J.H., Monks, A., Fisher, R.J., Shoemaker, R.H., and Melillo, G. (2005). Echinomycin, a small-molecule inhibitor of hypoxia-inducible factor-1 DNA-binding activity. Cancer Res. *65*, 9047–9055.

25. Lee, J.W., Bae, S.H., Jeong, J.W., Kim, S.H., and Kim, K.W. (2004). Hypoxia-inducible factor (HIF-1)alpha: its protein stability and biological functions. Exp. Mol. Med. *36*, 1–12.

26. Zhang, S.Q., Yang, W., Kontaridis, M.I., Bivona, T.G., Wen, G., Araki, T., Luo, J., Thompson, J.A., Schraven, B.L., Philips, M.R., and Neel, B.G. (2004). Shp2 regulates SRC family kinase activity and Ras/Erk activation by controlling Csk recruitment. Mol. Cell *13*, 341–355.

27. Ruthenborg, R.J., Ban, J.J., Wazir, A., Takeda, N., and Kim, J.W. (2014). Regulation of wound healing and fibrosis by hypoxia and hypoxia-inducible factor-1. Mol. Cells *37*, 637–643.

28. Jing, L., Li, S., and Li, Q. (2015). Akt/hypoxia-inducible factor-1α signaling deficiency compromises skin wound healing in a type 1 diabetes mouse model. Exp. Ther. Med. *9*, 2141–2146.

29. Hou, Z., Nie, C., Si, Z., and Ma, Y. (2013). Deferoxamine enhances neovascularization and accelerates wound healing in diabetic rats via the accumulation of hypoxia-inducible factor-1α. Diabetes Res. Clin. Pract. *101*, 62–71.

30. Mannell, H.K., Pircher, J., Chaudhry, D.I., Alig, S.K., Koch, E.G., Mettler, R., Pohl, U., and Krötz, F. (2012). ARNO regulates VEGF-dependent tissue responses by stabilizing endothelial VEGFR-2 surface expression. Cardiovasc. Res. *93*, 111–119.

31. Kontaridis, M.I., Liu, X., Zhang, L., and Bennett, A.M. (2002). Role of SHP-2 in fibroblast growth factor receptor-mediated suppression of myogenesis in C2C12 myoblasts. Mol. Cell. Biol. *22*, 3875–3891.

32. Alig, S.K., Stampnik, Y., Pircher, J., Rotter, R., Gaitzsch, E., Ribeiro, A., Wörnle, M., Krötz, F., and Mannell, H. (2015). The tyrosine phosphatase SHP-1 regulates hypoxia inducible factor-1α (HIF-1α) protein levels in endothelial cells under hypoxia. PLoS ONE *10*, e0121113.

33. Krötz, F., Engelbrecht, B., Buerkle, M.A., Bassermann, F., Bridell, H., Gloe, T., Duyster, J., Pohl, U., and Sohn, H.Y. (2005). The tyrosine phosphatase, SHP-1, is a negative regulator of endothelial superoxide formation. J. Am. Coll. Cardiol. *45*, 1700–1706.

34. Mannell, H., Pircher, J., Fochler, F., Stampnik, Y., Räthel, T., Gleich, B., Plank, C., Mykhaylyk, O., Dahmani, C., Wörnle, M., et al. (2012). Site directed vascular gene delivery in vivo by ultrasonic destruction of magnetic nanoparticle coated microbubbles. Nanomedicine (Lond.) *8*, 1309–1318.

35. Mykhaylyk, O., Sánchez-Antequera, Y., Vlaskou, D., Hammerschmid, E., Anton, M., Zelphati, O., and Plank, C. (2010). Liposomal magnetofection. Methods Mol. Biol. *605*, 487–525.